

# Redundancy of steel girder bridges

Autor(en): **Ghosn, Michel**

Objekttyp: **Article**

Zeitschrift: **IABSE reports = Rapports AIPC = IVBH Berichte**

Band (Jahr): **76 (1997)**

PDF erstellt am: **13.09.2024**

Persistenter Link: <https://doi.org/10.5169/seals-57464>

## **Nutzungsbedingungen**

Die ETH-Bibliothek ist Anbieterin der digitalisierten Zeitschriften. Sie besitzt keine Urheberrechte an den Inhalten der Zeitschriften. Die Rechte liegen in der Regel bei den Herausgebern.

Die auf der Plattform e-periodica veröffentlichten Dokumente stehen für nicht-kommerzielle Zwecke in Lehre und Forschung sowie für die private Nutzung frei zur Verfügung. Einzelne Dateien oder Ausdrucke aus diesem Angebot können zusammen mit diesen Nutzungsbedingungen und den korrekten Herkunftsbezeichnungen weitergegeben werden.

Das Veröffentlichen von Bildern in Print- und Online-Publikationen ist nur mit vorheriger Genehmigung der Rechteinhaber erlaubt. Die systematische Speicherung von Teilen des elektronischen Angebots auf anderen Servern bedarf ebenfalls des schriftlichen Einverständnisses der Rechteinhaber.

## **Haftungsausschluss**

Alle Angaben erfolgen ohne Gewähr für Vollständigkeit oder Richtigkeit. Es wird keine Haftung übernommen für Schäden durch die Verwendung von Informationen aus diesem Online-Angebot oder durch das Fehlen von Informationen. Dies gilt auch für Inhalte Dritter, die über dieses Angebot zugänglich sind.



# Redundancy of Steel Girder Bridges

**Michel GHOSN**

Associate Professor  
The City College of New York  
New York, NY, USA

Michel Ghosn received his Ph.D. in Civil Engineering from Case Western Reserve University, in 1984. He joined the City College of New York in 1985. His research interests are in the reliability and load modeling of bridge structures.

## Summary

This paper proposes a framework to include bridge redundancy during the design and evaluation of steel-girder bridges. Redundancy is defined as the capability of a bridge system to continue to carry loads after the failure or the damage of one or more of the bridge's main load carrying members. This paper illustrates how typical design-check equations could be modified by including system factors that account for the level of redundancy inherent in a particular steel bridge configuration. These system factors are calibrated using reliability techniques to ensure that bridge structural systems will provide acceptable levels of structural safety.

## 1. Introduction

The structural components of a bridge system do not behave independently, but interact with other components to form one structural system. Current bridge specifications generally ignore this system effect and deal with individual components. Since redundancy is related to system behavior, this study proposes a method to close the gap between a component by component design and the system effects. This is achieved by including system factors in the member design equations of bridge superstructures. The system factors are calibrated using reliability techniques based on the nonlinear behavior of steel-girder bridge configurations. This paper reviews the results of the analysis of steel bridges and illustrates how the calibration process is carried out.

## 2. Nonlinear analysis procedure

The behavior of typical steel I-beam bridges is analyzed using the Nonlinear Bridge Analysis program NONBAN [1]. The program uses a modified grillage analysis method to study the nonlinear behavior of typical bridge configurations. The discretization procedure required is typical for the grillage analysis method as described by Hambly or Zokaie and Imbsen [2,3].

NONBAN requires the linear and nonlinear material properties of each beam element. An element's linear elastic properties include the modulus of elasticity, the moment of inertia, the shear modulus, and the torsional constant. The nonlinear properties are represented by a moment versus plastic rotation curve. The moment versus plastic rotation curve is obtained from the



moment versus curvature relationship by multiplying the curvature by the length of the element. This assumes that the moment and curvature are constant over the length of the beam element.

The moment versus plastic curvature relationship for a steel member is obtained based on the experimental data assembled by Schilling [4]. The experimentally derived curve accounts for steel yielding including: the effect of residual stresses; the spread of yielding along the length of the beam element as the loading progresses; cracking or local crushing of the slab; permanent distortion of the cross sectional shape; and any other factor that causes permanent rotations. The moment curvature relationships for the transverse members representing the contribution of the concrete slab are obtained analytically from the stress-strain curves of the concrete and reinforcing steel bars using section equilibrium. Details about the program NONBAN and the modeling scheme used in this study are provided in Reference [1].

## 2. Model verification

The validity of the program NONBAN and the modeling scheme used to study the behavior of steel I-beam bridges is verified by comparing the results of NONBAN to those of two full-scale bridge tests. The first test was performed in Tennessee on a four-span continuous bridge [6]. The bridge consists of four steel W36x170 rolled I-beams at 2.5 m (8.25 ft) spacing supporting a 178 mm (7 in) deck slab. Sections over the piers have cover plates. Loads were placed to simulate one AASHTO HS-20 design truck [5] in each lane of the second span. Figure 1 shows a comparison between the field results published in reference [6] and the results of NONBAN. Excellent agreement is observed for the whole range of loading. This includes the prediction of the yielding load and the ultimate load.

The Nebraska laboratory test was performed on a full scale simple span 21 m (70 ft) bridge [7]. The bridge consists of three steel plate girders at 3m (10 ft) spacing supporting a 190 mm (7.5 in) deck slab. Loads were placed to simulate two side-by-side AASHTO HS trucks. The beams and the slab were built to act as composite sections. Figure 2 shows a comparison between the laboratory results published in reference [7] and the results of NONBAN. Excellent agreement is again observed although the test results show that the ultimate capacity was not reached because punching shear failure occurred in the slab slightly before ultimate load.

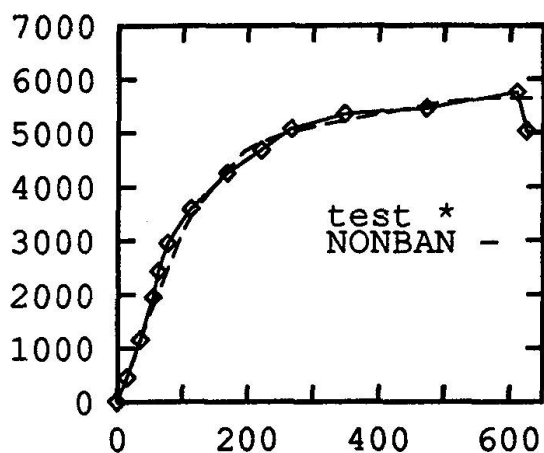


Fig. 1 Comparison of NONBAN to Tennessee's test [6].

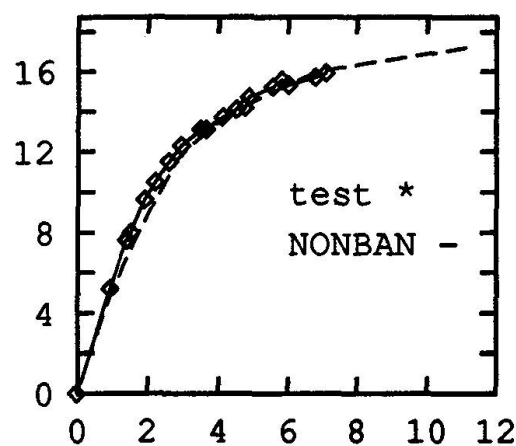


Fig. 2 Comparison of NONBAN to Nebraska's test [7].

The comparisons between the results of NONBAN and the two full scale bridge tests as well as other tests reported in reference [1] illustrate the validity of the program and the modelling scheme used in this study. The comparisons confirm that the moment-rotation curves developed in this study based on the experimental data proposed by Schilling [4] provide excellent representations of the actual behavior of steel bridge members.

### 3. Analysis of typical steel -girder bridge configurations

To study the behavior of typical steel I-beam bridge configurations several steel bridges are designed to cover typical span lengths and cross-sectional configurations. The bridges are designed to satisfy AASHTO's LFD criteria [5]. Simple span bridges as well as continuous two-span bridges with individual span lengths varying between 14 and 46 m ( 45 and 150 ft) are designed assuming that the deck is supported by 4, 6, 8 or 10 beams with beam spacing varying between 122 and 366 cm (4 and 12 ft). The concrete bridge decks are assumed to vary in depth between 19 and 22 cm (7.5 and 8.5 in) depending on the beam spacing. For each bridge configuration, section dimensions were chosen to satisfy AASHTO' s requirements for beam depths. The beams are assumed to be A-36 steel ( $f_y = 246$  MPa) while the deck's strength,  $f_c$ , is equal to 24 MPa (3.5 ksi).

The nonlinear analysis of these bridge systems is performed using NONBAN. The mesh discretization and models used in this study follow the guidelines given in reference [3]. The beams in the longitudinal direction account for the composite action between the slab and the I-beams. In addition, it is assumed that the bridges have no transverse diaphragms. Hence, the lateral distribution of the load is only affected by the transverse properties of the deck slab.

The dead load is assumed to be uniformly distributed along the length of each longitudinal member. All the longitudinal members are assumed to carry the same dead load. The live load is formed by AASHTO HS-20 vehicles placed longitudinally in the most critical design points. The base case assumes two side-by-side vehicles. No resistance nor load safety factor or dynamic impact factors are applied during the analysis. This is because the purpose of the incremental analysis is to evaluate the capacity of the bridge expressed in terms of how many HS-20 trucks it can carry before it fails. The effect of the dynamic impact is included at a later stage during the reliability analysis.

The AASHTO HS-20 vehicles are incremented until bridge system failure occurs. The load factor at which the system fails is defined as L<sub>Fu</sub>. L<sub>Fu</sub> gives the factor by which the weights of the initial HS-20 vehicles are multiplied to produce system failure. Failure of the bridge is assumed to occur when one main longitudinal member reaches a plastic hinge rotation equal to the maximum allowable plastic rotation. The maximum allowable plastic rotation corresponds to the value at which the concrete crushes or the steel ruptures. It is herein assumed that concrete crushing under transverse bending or in secondary members will only produce local failures. Therefore, no failures in the transverse direction are considered.

In addition to calculating the load factor corresponding to the ultimate capacity of the bridge system (L<sub>Fu</sub>), the load factor corresponding to the level at which the bridge becomes non-functional is recorded. It is assumed that a bridge becomes non-functional when the maximum live load displacement under a main longitudinal member reaches a value corresponding to the span length/100. The load factor corresponding to this displacement level is expressed by the variable L<sub>F100</sub>. The L/100 value is chosen because it is similar to the values at which many bridge field tests were stopped when the researchers observed potentially dangerous deflections.

Following the calculation of the ultimate capacity of the intact structure, a similar analysis is performed assuming damaged conditions. The damage scenario assumes that the external girder is so heavily damaged that it can no longer carry any load. This simulates a situation where the external girder is knocked out of service due to a collision or fracture. The incremental nonlinear analysis of bridge structures where the external member is assumed to be totally damaged is executed using the same assumptions stated above for the intact structures. The ultimate load capacity for a damaged bridge scenario is designated by the variable L<sub>Fd</sub>.

To provide a measure of a bridge's level of redundancy, the load factor at which the intact bridge system fails (L<sub>Fu</sub>), the load factor at which the bridge becomes dysfunctional (L<sub>F100</sub>) as well as the load factor for the damaged bridge scenario (L<sub>Fd</sub>) are compared to the load factor corresponding to the first member failure L<sub>F1</sub>. L<sub>F1</sub> in this case is calculated assuming linear elastic behavior of the bridge members. A linear elastic behavior is assumed in order to be consistent with current member oriented design and analysis procedures. Thus, the L<sub>F1</sub> factor represents the estimated bridge member capacity using current traditional member checking methods without consideration of the code-specified safety factors. The calculation of L<sub>F1</sub> is performed using the equation:



$$LF_1 = \frac{R - D}{DF_1 \cdot LL_{HS-20}}$$

where R is the member's unfactored moment capacity, D is the member's unfactored dead load,  $DF_1$  is the linear elastic distribution factor for the member assuming linear elastic behavior, and  $LL_{HS-20}$  is the total live load moment effect due to the HS-20 vehicles. The product  $DF_1 \cdot LL_{HS-20}$  correspond to the highest live load linear moment effect for any longitudinal member.

As an example of the results obtained, Table 1 gives the LFu, LF100, LFd and LF1 factors for the 46 m (150 ft) simple span bridges. Because redundancy is essentially a comparison between the system capacity and that of the individual members, the ratios of LFu/LF1, LF100/LF1 and LFd/LF1 are used as objective deterministic measures of bridge redundancy. These ratios are also shown in Table 1.

		4 beams		6 beams		8 beams		10 beams	
		LF	LF/LF1	LF	LF/LF1	LF	LF/LF1	LF	LF/LF1
4 ft	LFu	2.51	1.01	3.55	1.41	3.69	1.46	3.76	1.44
	LF100	2.51	1.01	3.13	1.25	3.25	1.29	3.36	1.29
	LFd	1.45	0.59	2.16	0.86	2.29	0.90	2.29	0.87
	LF1	2.48	-	2.52	-	2.52	-	2.62	-
6 ft	LFu	3.65	1.27	3.90	1.37	4.03	1.36	4.05	1.35
	LF100	3.34	1.16	3.51	1.23	3.68	1.24	3.70	1.23
	LFd	1.61	0.56	1.88	0.66	1.95	0.66	1.95	0.65
	LF1	2.88	-	2.85	-	2.97	-	3.00	-
8 ft	LFu	4.14	1.33	4.42	1.35	4.46	1.35	4.47	1.35
	LF100	3.74	1.20	4.03	1.23	4.09	1.24	4.09	1.24
	LFd	1.47	0.47	1.79	0.55	1.78	0.54	1.73	0.52
	LF1	3.12	-	3.26	-	3.31	-	3.31	-
10 ft	LFu	4.46	1.30	4.78	1.33	4.79	1.33	-	-
	LF100	4.14	1.21	4.45	1.24	4.47	1.24	-	-
	LFd	1.23	0.36	1.39	0.39	1.38	0.38	-	-
	LF1	3.43	-	3.59	-	3.59	-	-	-
12 ft	LFu	4.80	1.27	5.00	1.30	-	-	-	-
	LF100	4.52	1.20	4.74	1.23	-	-	-	-
	LFd	1.06	0.28	1.21	0.31	-	-	-	-
	LF1	3.77	-	3.85	-	-	-	-	-

**Table 1** Results of nonlinear analysis of 46 m bridge

#### 4. Sensitivity analysis

In addition to the analysis of the bridges described above, a parametric analysis is performed to study the sensitivity of the results to the assumptions made during the design of the bridge members and during the nonlinear analysis of the structural models. The simply-supported 46 m (150 ft) bridge with 6 beams at 240 cm (8 ft) is used as the base case for the sensitivity analysis.

The results of Table 2 show that the structural model used provides reasonably stable results. Changes in the  $LF_u/LF_1$ ,  $LF_{100}/LF_1$  and  $LF_d/LF_1$  ratios are significantly affected by changes in the moment capacity of the longitudinal girders and changes in the dead load. Other factors that are of importance are the moment capacities of the slab and the maximum plastic hinge rotation. Also, it is observed that the effect of changes in the deck slab capacities are insignificant for the intact bridge. Similarly, the presence of diaphragms at each support and the mid-span does not improve the results obtained for the intact bridges. On the other hand, placing a diaphragm at the bridge's mid-span and the strengthening of the deck slab improve the overall system capacity and redundancy of damaged bridges. It is also noted that, although a high increase in the assumed torsional rigidity of the longitudinal beams does not affect the results of the analysis significantly, an increase in the torsional rigidity of the members representing the deck slab produce a noticeable improvement in the  $LF/LF_1$  ratios especially for the damaged case. Other results show that increasing the bridge skew does not produce any significant change in the  $LF_u/LF_1$  ratio of the intact bridge although a reduction in the ratio of damaged bridges is observed. It is also noted that an increase in the longitudinal member capacities will decrease the  $LF/LF_1$  ratios.

The results of the simple span bridge are also compared to those of a continuous two-span bridge. The analysis of the continuous bridges shows that the two-span continuous bridges produce higher system redundancy only when the support is provided with sufficient levels of ductility in the negative bending region. This requires the use of compact steel sections over the interior supports.

	$LF_u$	$LF_{100}$	$LF_d$	$LF_1$	$LF_u/LF_1$	$LF_{100}/LF_1$	$LF_d/LF_1$
Base case	4.43	4.03	1.79	3.26	1.36	1.24	0.55
Fully composite	4.42	4.03	1.79	3.26	1.35	1.24	0.55
Double long. torsional constant	4.59	4.17	1.91	3.30	1.39	1.26	0.58
Double trans. torsional constant	4.69	4.16	2.11	3.30	1.42	1.26	0.64
Double long. moment of inertia	4.41	4.13	1.76	3.25	1.36	1.27	0.54
Double trans. moment of inertia	4.43	4.07	1.77	3.24	1.36	1.25	0.55
Double long. moment capacity	10.23	8.90	4.10	8.72	1.17	1.02	0.47
Double trans. moment capacity	4.51	4.08	2.02	3.26	1.38	1.25	0.62
Double dead load	1.71	1.51	0.00	1.07	1.60	1.42	0.00
Double maximum hinge rotation	4.86	4.03	2.31	3.26	1.49	1.24	0.71
30 degree skew	4.49	4.08	1.69	3.30	1.36	1.24	0.51
diaphragms at ends	4.42	4.04	1.82	3.26	1.36	1.24	0.56
diaphragms at ends & midspan	4.50	4.12	2.05	3.30	1.36	1.25	0.62

**Table 2** Results of Sensitivity Analysis.





## 5. Reliability analysis and calibration of redundancy factors

### 5.1 Reliability analysis

To perform the reliability analysis, statistical information on the loads applied on the bridge and the resistance of the system are required. In this study, the resistance of the intact system is expressed in terms of the load multipliers  $LF_u$  for the ultimate capacity,  $LF_{100}$  for the functionality criteria, and  $LF_1$  for member failure assuming linear elastic behavior. The load factors obtained from the nonlinear analysis express the capacity of the intact system to carry the live load. This capacity is a function of the applied dead load and the member resistance. Since these are random variables, then the capacity of the system is also random. For example, Equation 1 can be used to find the mean of  $LF_1$  and the COV given the means of  $R$  and  $D$ .  $DF_1$  and  $LLHS_{20}$  are taken to be deterministic variables. During the calibration of the AASHTO LRFD specifications, Nowak [8] found that the average member capacity of steel members is actually 1.12 times the nominal design capacity (resistance bias = 1.12). The steel member resistances are also associated with a coefficient of variation COV equal to 10%. In addition, Nowak [8] assumes that the dead loads applied on the structure will have a bias that varies between 1.03 and 1.05 with a COV between 8% and 10%. Based on these observations it is herein assumed that on the average, the total combined dead load effects will have a bias on the order of 1.05 and a COV on the order of 10%.

Nowak [8] also assumes that the maximum lifetime (75 year) live loads (including dynamic impact) produce maximum moments which can be represented as multiples of the effects of the HS-20 trucks. Different factors are obtained depending on the span length. For example, for a 46 m (150 ft) bridge a factor equal to 2.01 is found. The 2.01 factor accounts for the dynamic impact as well as the static moment effect. Nowak [8] also assumes that the applied live load (including impact effect) is associated with a coefficient of variation equal to 19%. The 75 year lifetime load is used herein to find the reliability of the system against total collapse and against first member failure. Similar factors are provided for the two-year return period. These are used for the functionality criteria and the damaged condition.

The reliability calculations performed herein use the statistical information given above and assume that the  $LF_1$  factor follows a lognormal distribution while the applied load follows a Gumbel distribution. The calculation of the reliability of the whole system assumes that  $LF_u$  follows a lognormal distribution and is associated with the same bias as that of  $LF_1$  and the same COV. This assumption is somewhat subjective but is based on the observation made by Cornell [10] about the relationship between the member resistances and the system's resistance. On the other hand, it is well known that the COV of the system is generally smaller than the COV of the individual members. However, this assumes that the structural model and system analysis process is exact. To account for the uncertainties in the structural modelling process while performing a nonlinear analysis, it is herein suggested to conservatively use a COV on  $LF_u$  equal to the COV on the member resistances as represented by  $LF_1$ . The same logic is followed while calculating the reliability index for the functionality and the damaged limit states.

The safety indices obtained for the 46 m (150 ft) bridges analyzed in this study for the intact ultimate capacity,  $\beta_u$ , and the functionality limit state,  $\beta_s$ , as well as the damaged bridge,  $\beta_d$ , conditions are given in reference [1]. These values are also compared to the member safety indices,  $\beta_{\text{member}}$ .

## 5.2 Determination of redundancy criteria

Reference [1] gives the reliability indices obtained in this study for the simple span steel bridges. The results show that for the ultimate limit state, the system reliability,  $\beta_u$ , is on the average higher than the member reliability,  $\beta_{\text{member}}$ , by 0.98 for all the 46 m simple span bridges considered. This means that  $\Delta\beta_u$  ( $\beta_u - \beta_{\text{member}}$ ), which is defined as a probabilistic measure of redundancy, is on the average equal to 0.98. Therefore, it is proposed to use a  $\Delta\beta_u$  value of 1.0 (obtained by rounding up 0.98) as the redundancy criterion for the ultimate limit state. Thus, a bridge is defined as sufficiently redundant if the reliability index of the system is higher than that of the member by at least 1.0.

The average  $\Delta\beta_s$  ( $\beta_s - \beta_{\text{member}}$ ) value obtained for the 46 m simple span bridges studied for the functionality limit state is 0.91. Therefore, a  $\Delta\beta_s$  value of 0.95 is used as the redundancy criterion for the functionality limit state. For the damaged limit state, the average difference  $\Delta\beta_d$  ( $\beta_d - \beta_{\text{member}}$ ) between the damaged system's safety index and the member safety index of the intact system is -2.04. Therefore, a value of -2.0 is used as the redundancy criterion for damaged bridges. The redundancy criteria chosen will be used in the next section as the target values during the calibration of the proposed system factors.

## 5.3 Calibration of system factors

System factors are calibrated such that bridges having configurations that do not provide sufficient levels of redundancy are penalized by requiring their individual members to provide higher levels of safety than those of bridges with sufficiently high levels of redundancy. On the other hand, bridges with high levels of redundancy are rewarded by allowing a lower level of member safety. This is performed by introducing system redundancy factors in the design or safety-check equations. The proposed format is such that:

$$\phi_s \phi R = \gamma_d D + \gamma_l L \quad (2)$$

where  $\phi_s$  is the system redundancy factor,  $\phi$  is the member resistance factor,  $R$  is the resistance capacity of the member,  $\gamma_d$  is the dead load factor,  $D$  is the dead load effect,  $\gamma_l$  is the live load factor, and  $L$  is the live load effect on an individual member (including dynamic impact). When  $\phi_s$  is equal to 1.0, Equation (2) becomes the same as the current design equation. If  $\phi_s$  is greater than 1.0 it indicates that the system's configuration provides sufficient level of redundancy. When it is less than 1.0 then the level of redundancy is not sufficient.

The redundancy criteria for  $\Delta\beta_u$ ,  $\Delta\beta_s$  and  $\Delta\beta_d$  chosen in the previous section are used to calibrate system redundancy factors for each bridge configuration analyzed in this study. The procedure is performed such that bridges that produce  $\Delta\beta_u$ ,  $\Delta\beta_s$  and  $\Delta\beta_d$  values less than the target values will be subjected to higher safety factors on their member resistances. The object is to increase their members' safety indices by the amounts  $\Delta\beta_u - \Delta\beta_{u \text{ target}}$ ,  $\Delta\beta_s - \Delta\beta_{s \text{ target}}$ , and  $\Delta\beta_d - \Delta\beta_{d \text{ target}}$ . Different  $f_s$  values are calculated for each of the limit states studied.

Values of  $f_s$  factors for the 46 m simple span bridges with two-lanes of loading are shown in Table 3 for the three limit states studied. The results show that for a given beam spacing, the  $f_s$  factor (i.e. the bridge redundancy) increases as the number of beams is increased. This increase, however, reaches a plateau at 6 beams. Thus, no major improvement in bridge redundancy is observed when the number of members is increased beyond 6 beams.





		4 beams	6 beams	8 beams	10 beams
4 ft	ultimate	0.84	1.03	1.05	1.05
	functi.	0.89	1.01	1.03	1.03
	damage	0.87	1.12	1.13	1.13
6 ft	ultimate	0.97	1.00	1.00	1.00
	functi.	0.97	1.00	1.00	1.00
	damage	0.84	0.95	0.96	0.95
8 ft	ultimate	0.99	1.00	1.00	1.00
	functi.	0.98	1.00	1.00	1.00
	damage	0.74	0.84	0.83	0.81
10 ft	ultimate	0.98	0.99	0.99	
	functi.	0.98	1.00	1.00	
	damage	0.58	0.63	0.62	
12 ft	ultimate	0.96	0.97		
	functi.	0.98	0.99		
	damage	0.46	0.52		

**Table 3** System factors for bridge redundancy

The results also show that for a given number of beams, the  $\phi_s$  factor increases as the beam spacing is increased from 1.2 m to 2.4 m (4 ft to 8 ft). However, the factor decreases as the beam spacing is increased beyond 2.4 m. This trend is explained by the fact that, for narrow bridges, all the beams are almost equally loaded and there is no reserve strength available. Hence, if one beam fails all the beams will quickly follow suit. However, as the beam spacing is increased, the load distribution is uneven and the least loaded members will pick up the load as the most heavily loaded member fails. As the spacing becomes very large, the capacity of the slab to transfer the load decreases and damage to the members under the applied load occur before a complete transfer to the other members is possible. This observation is evident because the nonlinear analysis performed herein considers the possibility of system damage before the formation of a plastic mechanism. Similar trends are observed for the ultimate limit state, the functionality limit state, or the damaged limit state. The trends are however the sharpest for the damaged limit state.

## 6. Conclusions

A method to account for bridge redundancy during the design and evaluation of bridge systems is proposed. The method consists of introducing system factors in the member design and evaluation equations. The factors are calibrated such that bridges that do not have sufficient levels of redundancy are penalized by requiring their members to have higher levels of safety than comparable redundant designs. On the other hand, bridges with high levels of redundancy are rewarded by allowing their members to have lower safety factors than normally required by current design and evaluation methods. Further work is underway to account for the results of the parametric analysis in the proposed framework.

## Acknowledgements

The work presented herein is part of a study supported by NCHRP project 12-36/2 entitled "Redundancy in Highway Bridge Superstructures". The opinions presented in this paper are those of the author and do not necessarily represent the views of NCHRP, TRB or FHWA. The contributions of Dr. Fred Moses and Mr. Linzhong Deng are gratefully acknowledged.

## References

1. GHOSN M. and MOSES F., "Redundancy in Highway Bridge Superstructures" Report NCHRP 12-36, TRB, Washington DC, March 1994.
2. HAMBLY, E.C., "Bridge Deck Behaviour", Chapman and Hall, Ltd., London, 1976.
3. ZOKAIE T., OSTERKAMP, T.A., and IMBSEN R.A., "Distribution of Wheel Loads on Highway Bridges", Final Report, NCHRP project 12-26/1, March 1991.
4. SCHILLING C.G., "A Unified Autostress Method", Project 51, Development of Design Specifications for Continuous Composite Plate-Girder Bridges, American Iron and Steel Institute, November 1989.
5. AASHTO, Standard Specifications for Highway Bridges, 15th. Ed., Wash. DC, 1992.
6. BURDETTE E.G. and GOODPASTURE, D.W., "Full Scale Bridge Testing - An Evaluation of Bridge Design Criteria", University of Tennessee, December 1971.
7. KATHOL S., AZIZINAMINI, A. and, LUEDKE, J., "Strength Capacity of Steel Girder Bridges", NDOR Research Project No. RES1 (0099) P469, Nebraska Department of Roads, February 1995.
8. NOWAK, A.S., "Calibration of LRFD Bridge Design Code", NCHRP 12-33, May 1992.
9. AASHTO, LRFD Bridge Design Specifications, First Edition, Washington DC, 1994.
10. CORNELL, C. A., "Risk-Based Structural Design", Proceedings of a Symposium on Risk Analysis, Department of Civil Engineering, University of Michigan, Ann Arbor, MI, August 1994.

Leere Seite  
Blank page  
Page vide